

## Morphological changes probed as rheokinetics of whisker- and unfilled polymer blends

Anders L. Persson and Hans Bertilsson\*

Department of Polymeric Materials, Chalmers University of Technology,  
S-412 96 Göteborg, Sweden

(Received 3 April 1997; revised 27 October 1997; accepted 1 December 1997)

The rheological time dependencies of both whisker-filled (composites) and unfilled PE/PIB and SAN/PA6 blends were studied as functions of composition and shear history. A three-step experiment of steady dynamic–steady shear was designed. Rupture and formation of the morphology in batch-compounded blends/composites was conveniently and accurately studied in the first steady shear. The second step emphasises morphological sensitivity in blends close to phase inversion. During the oscillation phase metamorphosis and whisker transport were noticed. The third step together with microscopy studies confirmed these observations. © 1998 Elsevier Science Ltd. All rights reserved.

(Keywords: filled immiscible polymer blend; interpenetrating network; aluminum borate whiskers)

### INTRODUCTION

Thermoplastic polymer blends constitute a rapidly growing group of materials of great technical potential. However, there is usually a limited processing window that gives attractive property profiles to these materials. Several parameters need to be mastered to achieve desired property profiles, interfacial tensions, viscosities, elasticities and volume contents are fundamental parameters to control. The importance of the processing route has been stressed by several authors<sup>1–3</sup>. Also, the post-processing thermal treatment plays a very important role in determining the phase structure<sup>4–6</sup>. Knowledge of the kinetics is especially crucial when the polymers are of about equal volume contents because then the phase continuity may be altered, which has a strong influence on the properties of the material. Fortunately there are ways to reduce the importance of processing, for instance compatibilisation, in which a compatibiliser, usually a copolymer, stabilises the morphology. However there are only a limited number of blends that may be compatibilised in this way. An alternate approach is to use a filler to modify the phase structure. We have earlier shown<sup>7,8</sup> that addition of whiskers to immiscible blends may change their morphology from suspension-like to co-continuous. These whisker-filled blends involve profound processing-related difficulties as the number of morphological degrees of freedom increases with addition of another phase.

Much work on the rheology of polymer blends has been carried out using capillary rheometers. Han<sup>9</sup> showed that if there is a viscosity difference between the polymers, a channel flow creates a sheath-core morphology. Therefore, one must not use a velocity profile for homogeneous melts. Use of a rotational rheometer with cone and plate gives a more attractive shear field. The shear rate is constant throughout the sample and the deformation mode is then well defined.

In this work we have used previously characterised blends and composites based on HDPE/PIB with aluminum borate whiskers as the solid<sup>10</sup>. The polyolefin blend's interfacial tension is very low (0.49 mN/m) at the processing temperature, resulting in sufficiently slow coalescence to facilitate morphological snapshots. Furthermore, the similarity of the polyolefins' surface energetics gives polymer–whisker interactions of comparable strength. Also the well-characterised composite of SAN/PA6/W<sup>7</sup> that easily forms co-continuous structure was used. A rotational viscosimeter with cone and plate was used to study the rheokinetic response to steady shear as a function of the composition. The relaxation behaviour was studied in dynamic mode and the viscosity was finally studied as a function of the rheothermal history of the sample.

### EXPERIMENTAL

The materials used were polyethylene (PE), DMDS 7015 from Neste, which is a high density grade with  $M_n$  and  $M_w$  of 17 and 54 kg mol<sup>-1</sup>, respectively, and two different polyisobutylenes (PIB). The PIBs were purchased from Scientific Polymer Products. According to the supplier PIB1 has an  $M_v$  of 400 kg mol<sup>-1</sup> and PIB2 an  $M_v$  of 85 kg mol<sup>-1</sup>. We found  $M_n$  and  $M_w$  to be 38 and 384 kg mol<sup>-1</sup> for PIB1, and 12 and 101 kg mol<sup>-1</sup> for PIB2. The molecular mass distributions were determined by size exclusion chromatography with polyethylene and polystyrene standards in 1,2,4-trichlorobenzene and tetrahydrofuran for PE and PIB, respectively. Aluminum borate whiskers (Al<sub>2</sub>O<sub>3</sub>)<sub>9</sub>(B<sub>2</sub>O<sub>3</sub>)<sub>2</sub>, Alborex G, are single crystals with diameters of 0.5–1 μm, length of 10–30 μm, density of 2.93 g cm<sup>-3</sup> and a specific surface area of 2.5 m<sup>2</sup> g<sup>-1</sup>. The whiskers have excellent mechanical properties as well as thermal and chemical stability. They were provided by Shikoku Chemicals Corp. Densities at 170°C are 0.774, 0.717 and 2.92 g cm<sup>-3</sup> for PE, PIB and whiskers, respectively. Polyamide 6, Ultramid B3, was used in blends and composites with poly(styrene-co-acrylonitrile), Luran 378 P.

\* To whom correspondence should be addressed.

**Table 1** Recipes of the compounded blends and composites

	Plastics	v/o	$m_{\text{PIB}}$ (g)	$m_{\text{PIB+W}}$ (g)	$m_{\text{PE}}$ (g)	$m_{\text{PE+W}}$ (g)	$m_{\text{W}}$ (g)
B1	PIB1/PE	53.6/46.4	20.72		19.35		
B2	PIB1/PE	73.0/27.0	20.02		11.61		
B3	SAN/PA6		42.0*		18.0**		
C1	PIB1-W	95.6-4.4	39.38				7.32
C2	PIB2-W	95.6-4.4	39.38				7.32
C3	PE-W	95.0-5.0			36.76		7.32
C4	C1/PE	52.6(2.3)/45.1		23.95	18.85		
C5	C1/PE	70.8(3.1)/26.1		33.19	11.20		
C6	C1/PE	32.8(1.4)/65.8		18.08	33.21		
C7	C1/PE	11.4(0.5)/88.1		4.89	34.64		
C8	PIB1/C4	52.2/45.5(2.3)	20.19			22.61	
C9	C2/PE	52.6(2.3)/45.1		23.95	11.20		
C10	SAN/PA6-W		35.0*		15.0**		21.4
C11	SAN/PA6-W		15.0*		35.0**		21.4

The volume fractions in column three refer to the molten state at 170°C, e.g. C7 consists of 11.4 v/o PIB1, 0.5 v/o whiskers and 88.1 v/o PE. \* and \*\* refer to the mass of SAN and of PA6, respectively

Both were provided by BASF. Ultramid B3 had an  $M_n$  of 18 kg mol<sup>-1</sup> and a viscosity  $\eta_a(\dot{\gamma} = 1000 \text{ s}^{-1}, 235^\circ\text{C})$  of 270 Pa s and Luran 378 P had a 35% acrylonitrile content with MFI = 1.5.

Compounding of the blends and composites was done in a 50-cc Brabender AEV 330 plasticorder at 170°C for polyolefins and 235°C for SAN/PA6 for 5 min at 50 rpm, corresponding to shear rates up to 60 s<sup>-1</sup>. The high-viscosity polymer was plasticised before the second polymer was added. Whiskers for the ternary composites were added from precompounded composites with up to five v/o whisker loading unless otherwise noted. SAN, PA6 and whiskers were dried before compounding and were kept dry until further use. The blends and composites are presented in Table 1.

A Rheometrics RDA II instrument was used for the rheological studies. Parallel plates of 25 mm diameter were used to establish the dynamic flow curves of the pure polymers and their single-polymer composites, whereas cone and plate fixtures of 25 mm diameter were utilised for the filled and unfilled blends. The PIBs were run at 170 and 100°C and PE at 170 and 140°C; all other runs on polyolefins were performed at 170°C. The samples were heated at 170°C for 4 min and then deformed to the required circular shape. After this they were left at rest for 10 min before any shearing took place. SAN, PA6 and their blends and composites were all characterised at 235°C. The first sequence of the three-step experiment was steady shear at 1.0 s<sup>-1</sup>, followed by harmonic oscillation at low strain amplitude. The switch from steady to dynamic mode took 40–70 s. The third step was once again steady shear where the viscosity was sampled for 4.1 s in 5-s intervals. An average of the 4.1-s measurement results was presented as the viscosity, e.g. the first measured data point given after 6 s includes data sampled during the preceding 4.1 s. To change from steady to dynamic mode required that the upper fixture was in its reference position, i.e. the first step of steady shear was restricted to an integer number of revolutions. Cone and plate fixtures were used for the three-step sequence. A complementary three-step experiment where the samples were left at rest in the second step was used to study the influence from the oscillation.

Scanning electron microscopy (SEM) was done on a Zeiss DSM 940A. Samples were prepared by steady shear in

a rotational rheometer with cone and plate fixtures. The oven was opened wide to give as rapid cooling as possible with unforced cooling. It took approximately 1 min to reach crystallisation temperature for the PE before the disc could be peeled off. Circle sector-shaped samples were prepared by cryo-fracturing of the discs. The PIB phase was extracted by cyclohexane from these samples. This was followed by gold-sputtering of the residue.

## RESULTS AND DISCUSSION

Flow curves of the blend constituents are presented in Figure 1. The polyolefin curves are clearly separated in the shear rate range of interest here. There is a high viscosity ratio between PIB1 and PE and a small viscosity difference between PE and PIB2. The polyolefin blend (B2) and composite (C5) were primarily designed to be close to the point of phase inversion, while reference blends and composites should have a dispersion-like morphology (B1, C4 and C6–C9). In the available literature one can find

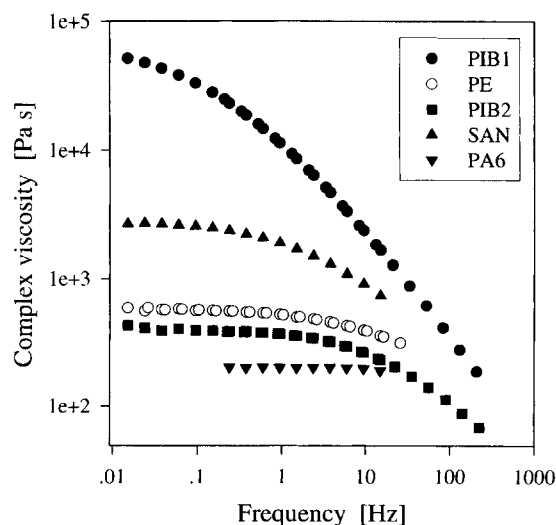


**Figure 1** Flow curves of the utilized plastics. For SAN and PA6 the temperature was 235°C; for PE it was 170 and 140°C, while it was 170°C and 100°C for PIB1 and PIB2. Both polyolefins are shifted to 170°C

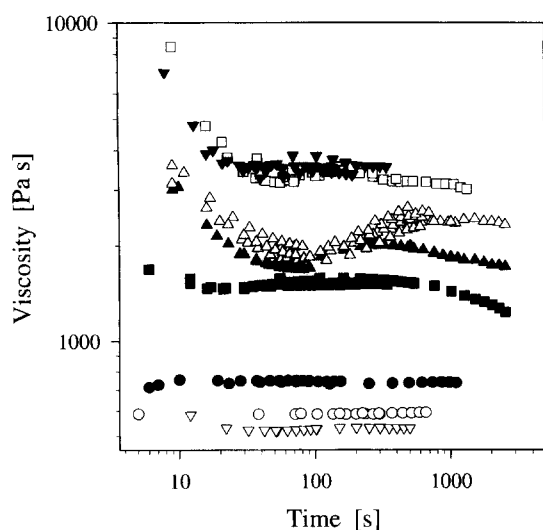


**Figure 2** Rheokinetics at  $1 \text{ s}^{-1}$  shear rate for various samples: PE  $\circ$ , C7 (PIB1(W)/PE, 11.4(0.5)/88.1)  $\bullet$ , C6 (PIB1(W)/PE, 32.8(1.4)/65.8)  $\blacksquare$ , C4 (PIB1(W)/PE, 52.6(2.3)/45.1)  $\blacktriangle$ , B2 (PIB1/PE, 73.0/27.0)  $\square$ , C5 (PIB1(W)/PE, 70.8(3.1)/26.1)  $\blacktriangledown$ , B1 (PIB1/PE, 53.6/46.4)  $\triangle$ , C9 (PIB2(W)/PE, 52.6(2.3)/45.1)  $\nabla$ .

several different methods of achieving phase inversion<sup>11</sup>. Here we chose the frequently confirmed expression by Jordhamo *et al.*<sup>12</sup>, formulated as equation (1):

$$\frac{\eta_1 \phi_2}{\eta_2 \phi_1} = 1 \quad (1)$$

The viscosities of the components are designated  $\eta_1$  and  $\eta_2$  and their volume fractions by  $\phi_1$  and  $\phi_2$ .

In *Figure 2* the viscous response to steady shear is displayed for Brabender-compounded blends and composites. Pure polyethylene is unaffected by prolonged shearing and so is C7. At a PIB content of 32.8 v/o plus 1.4 v/o whiskers, a moderate viscosity drop for around 20 s appears followed by a plateau region that ends with a pronounced viscosity decrease. The initial viscous drop is probably due to deformation of the dispersed PIB phase into a more elongated shape. Eventually these domains break up to form smaller and more spherical domains that represent a more viscous morphology. The dispersed character of the PIB phase can be seen in *Figure 3*. After the equilibrium size distribution has been reached the viscosity drops again. This may be explained by the formation of local whisker-PIB jams, seen as large cavities in *Figure 3b*, since the whisker loss from the PE matrix reduces its viscosity. For the higher PIB contents drastic viscosity changes are seen. From our earlier work on PIB/PE blends<sup>10</sup> we know that the starting morphologies of blends B1 and B2 and composites C4 and C5 are co-continuous. *Figure 4a* shows how the former continuous PIB phase in blend B1 (PIB1/PE, 53.6/46.4) has been ruptured during the start-up of steady shear to form discrete domains elongated in the radial direction. With cone and plate fixtures the shear rate is constant throughout the gap. Hence there should also be an orientation in the tangential direction. Thus the PIB domains must be dis-shaped, which corresponds to a minimised viscosity, as discussed earlier<sup>10</sup>. Prolonged shearing gives a viscous increase caused by fractionation of the stretched PIB domains. Still discrete but smaller and more spherical PIB domains are seen in *Figure 4b*, where the sample was sheared to the viscous plateau. Similar viscous increase has been observed<sup>13</sup> after a step increase of shear rate when

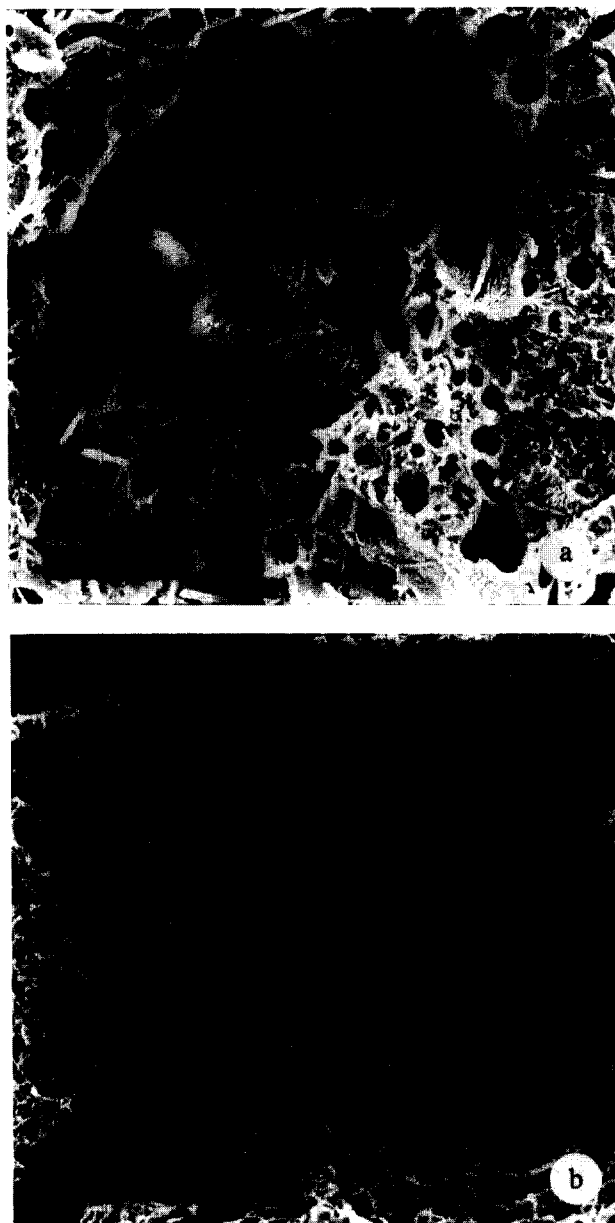


**Figure 3** SEM micrographs from fracture surfaces of C6 (PIB1(W)/PE, 32.8(1.4)/65.8), sheared at  $1 \text{ s}^{-1}$  shear rate during (a) 88 and (b) 2018 s

large elongated domains break up into smaller and more spherical ones. From our previous work we know that the 73.0/27.0, B2 blend forms a coherent structure of PE clusters in the PIB matrix after compounding followed by unforced cooling, which together with the 10 min of annealing sets the starting morphology. In approximately 40 s of steady shear the viscosity drops almost three times. This is caused by the fibrillation shown in *Figure 5* of the collapsed PIB-extracted sample. The extremely elongated PE phase acts as an internal lubricant for the blend. This is often found for blends with large viscosity ratios<sup>3,14,15</sup>. In C4 and C5, where whiskers are included, the pattern is repeated with minor variations. First, the viscosity drops more rapidly due to the inherent orienting effect from the large aspect ratio whiskers, which produces the elongated PIB and PE phases. It is noteworthy that the rheokinetic effect is similar despite different whisker hosts, visualised in *Figure 6a,b*, where all the free whiskers in *Figure 6a* indicate PIB absorption, whereas the PE phase hosts the whiskers in *Figure 6b*. *Figure 6* also illustrates the extreme

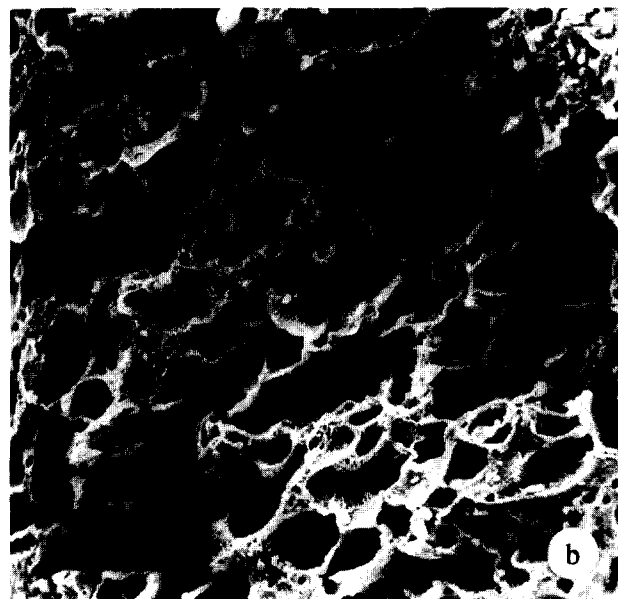
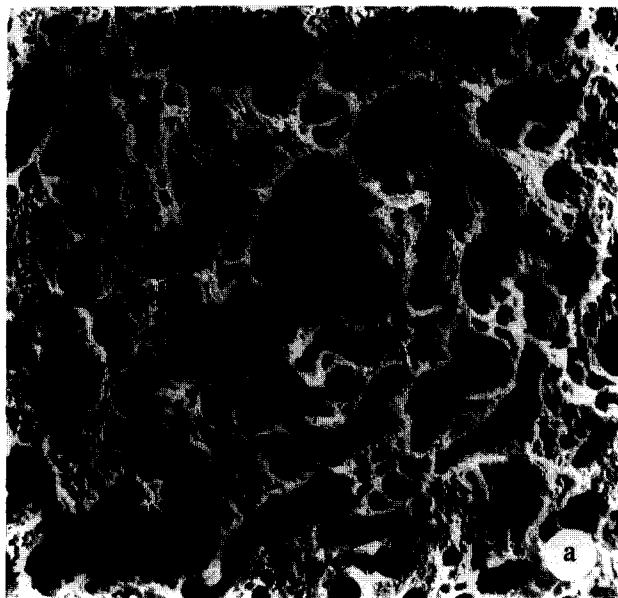


**Figure 4** SEM micrographs from fracture surfaces of B1 (PIB1/PE, 53.6/46.4), sheared at  $1 \text{ s}^{-1}$  for (a) 71 and (b) 722 s. The arrows indicate the radial direction of the disc-shaped samples

lamellar structure achieved with whiskers that give an even lower viscosity in spite of the viscous increase that follows when a filler is added to a homogeneous matrix. Secondly, the whiskers conserve and maintain a low viscosity morphology, which is seen from the reduced time to reach the viscous plateau in *Figure 2*. Further, the viscous steps from minimum to plateau are much lower than for the pure blends. For blends and composites with smaller viscosity ratio the potential of morphologically induced viscosity changes is much smaller. This can be seen for composite C9 in *Figure 2* that shows similar but weaker rheokinetic behaviour.

Pure PIB1 was too viscous to run in rotational rheometer at  $1 \text{ s}^{-1}$  shear rate. The sample was squeezed out of the gap.

A linked three-step experiment exemplified in *Figure 7* contributes significant information on the time-scale of the morphological changes that take place. To assure similar thermo-rheological starting conditions for the samples, they were either sheared to their viscous minimum or to the

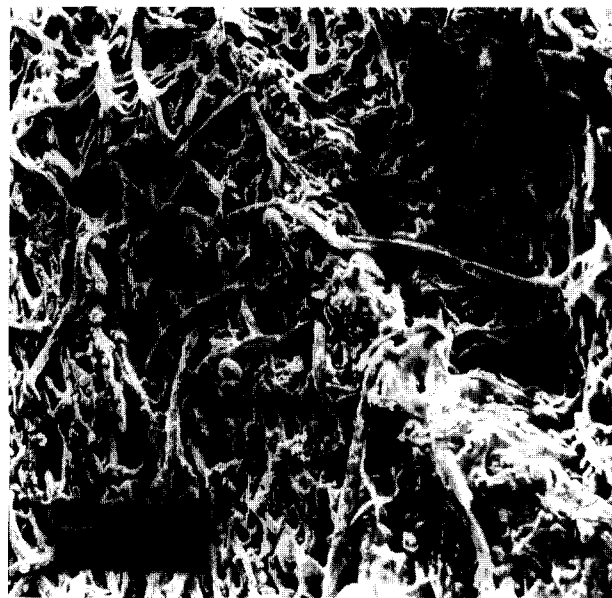


**Figure 5** SEM micrograph of the fracture-surface of B2 (PIB1/PE, 73.0/27.0) sheared 52 s at  $1 \text{ s}^{-1}$

plateau region. Then the instrument was switched to dynamic mode with low strain amplitude followed by another steady shear sequence for about 50 s. The minimum sampling time at  $1 \text{ s}^{-1}$  shear rate is 4.1 s for this instrument. We chose a time delay of 0.9 s between measurements. The instrument calculates the average value for the sampling time. Thus, the start-up viscosity of step three is actually much higher than the one presented here. To check if there are substantial degradation processes active during the hour that the experiments last we ran samples in dynamic mode for a prolonged time.

Possible morphological effects induced by the oscillation were tested for by comparing the start-up viscosity in the third step with samples left at rest during stage two. No significant difference was found.

As shown in *Figure 8*, whisker-filled PIB1 loses stiffness indicating degradation by unzipping of monomers, which is a likely response to prolonged heating<sup>16</sup>. The polyethylene shows a drastic stiffness increase at about 7000 s and the morphologically induced stiffness increase for the filled blend is accelerated after 5000 s. This is in accordance with observed PE behaviour in air<sup>17</sup>, giving molecule enlargement by oxidation at the fringe of the sample. The shorter time scale for the filled blend may be caused by synergistic degradation effects of the polyethylene, e.g. redistribution of a stabiliser. The conclusion from the degradation tests is that no severe degradation takes place during the duration of the three-step experiments.

*Figure 9* pertains to the dynamic stage of the three-step experiment with the blends/composites that were close to co-continuity, i.e. close to 50/50 v/o or fulfilling equation (1). These plots illustrate the influence of the shearing time, i.e. if shearing was terminated at the viscosity minimum or on the plateau. Small differences are seen: apart from C4, the sample for which the shearing was terminated on the plateau has the higher stiffness. It should be kept in mind that a cone and plate rheometer is very sensitive to thermal instability because of its narrow gap compared to the dimensions of the fixtures. Thus, the absolute values should be treated with some caution. However, the stiffness increase is undoubtedly more rapid for the composites

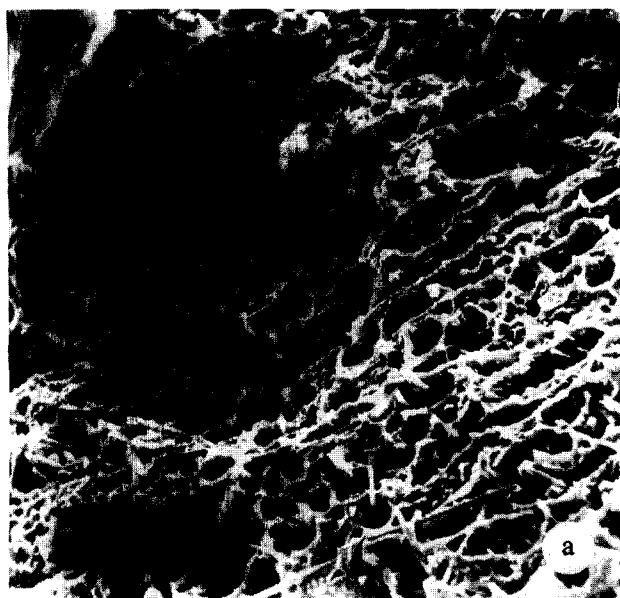


**Figure 6** SEM micrographs from fracture surfaces of PIB1(W)/PE composites in ratios (a) 52.6(2.3)/45.1 (C4) that were sheared for 71 s at  $1 \text{ s}^{-1}$  and (b) 70.8(3.1)/26.1 (C5) for 36 s. The arrows indicate the radial direction of the disc-shaped samples

than for the blends and their stiffening continues much longer than their unfilled equivalents.

Stage two results for all the blends and composites that were pre-sheared to their viscosity minima are presented in *Figure 10*. Some recovery processes take place for the blends and composites that were close to equal volume ratios or fulfilled equation (1). A clearer picture of the morphological kinetics appears if the sample stiffness is evaluated at different time intervals using the data presented in *Figure 10*. The results are shown in *Figure 11*, which shows that morphological changes are almost exclusively present in the samples with the higher PIB contents. For instance, at 70.8 v/o PIB1 (C5) the stiffening is more rapid than for the 52.6 v/o PIB1 (C4) composite. Furthermore, the stiffness of C4 approaches the rule of mixtures (straight line between PE-W and PIB1-W) after 1 h, and it continues to increase while C5 reaches levels well above the rule of mixtures.

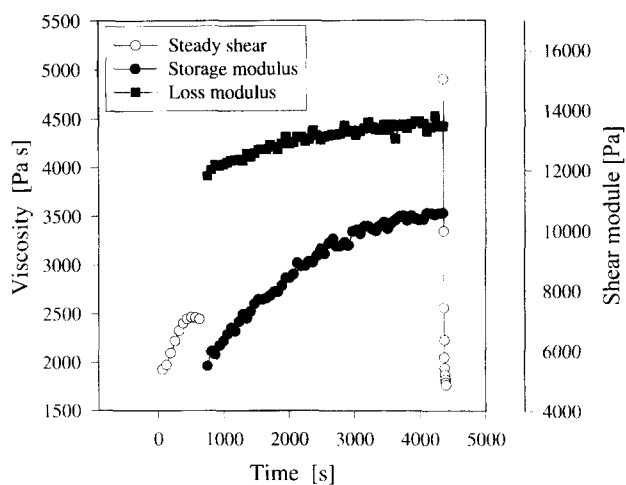


**Figure 7** Rheokinetics of B1 (PIB1/PE, 53.6/46.4) subjected to  $1 \text{ s}^{-1}$  steady shear for 622 s, sampled every 62nd second, followed by 1 h of harmonic oscillation at 1 Hz and 0.5% strain amplitude. The sequence was concluded with  $1 \text{ s}^{-1}$  steady shear for 52 s

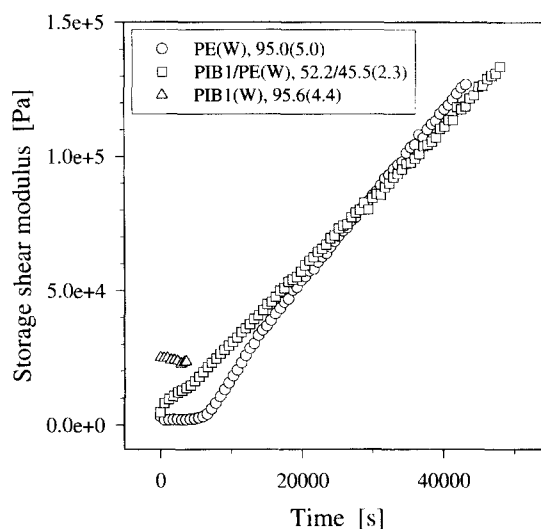


**Figure 8** Long-term stiffness changes

The photomicrographs in *Figure 12* of the equivalent blends indicate that the stiffening was caused by diametrically opposite processes. The 53.6 v/o PIB1 blend reforms the continuity of the ruptured PIB phase and continuously improves its co-continuous structure, while the elongated PE phase seen in *Figure 5* breaks into discrete particles without structural strength when the 73.0 v/o PIB1 is extracted. With discrete PE particles the overall stiffness reached after approximately 1000 s is mainly determined by the PIB1 matrix. For B1 at least 3000 s is required to reach this equilibrium morphology. The whisker-filled blends show similar behaviour with different time scales, which can be seen in *Figures 10 and 11*. When B1 stops stiffening, the whisker-filled C4 still continues to stiffen due to the delaying transport of whiskers by the high viscosity PIB1 phase known to host the whiskers<sup>10</sup>. For C5 the initial stiffening accounts for most of the change. This may be caused by localised stress concentrations in the whisker-supported continuous PE phase. The whiskers work as a skeleton for the PE phase but without joints, and when the flow stops the reduction of interfacial area starts leading to breakup of the PE phase. At the whiskers' encountering

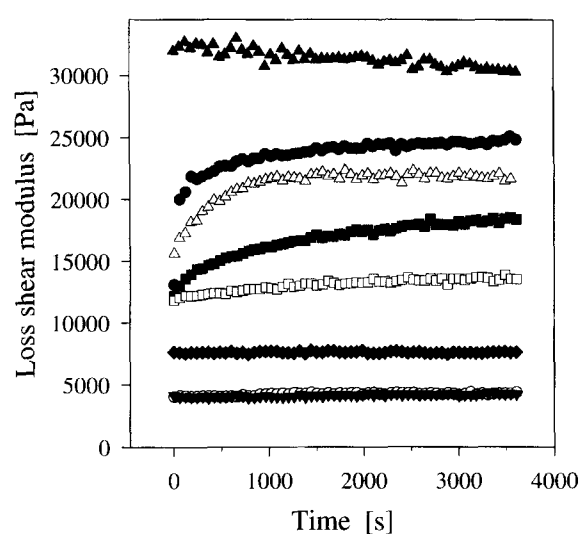
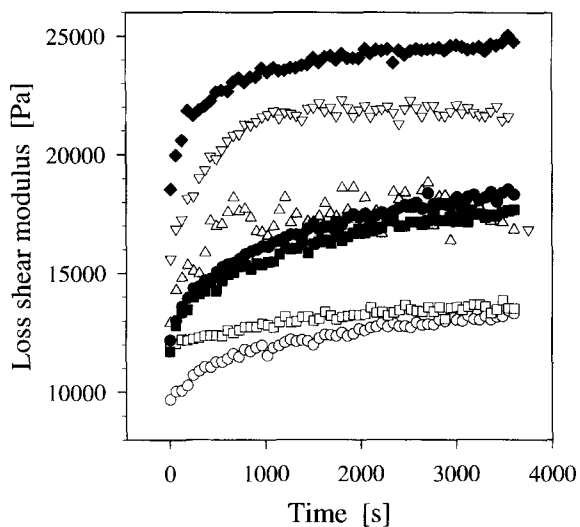
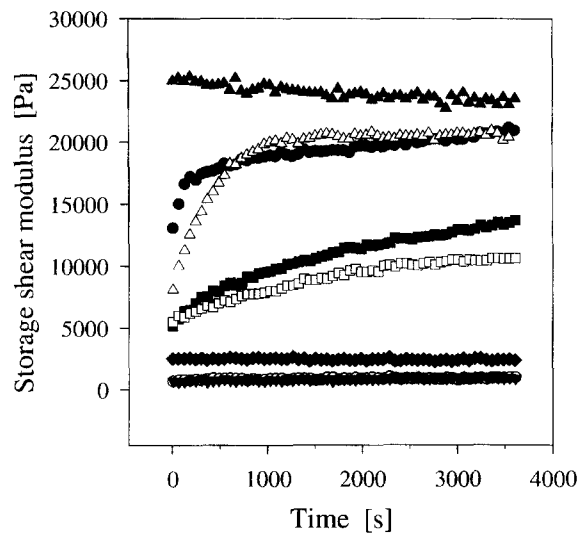
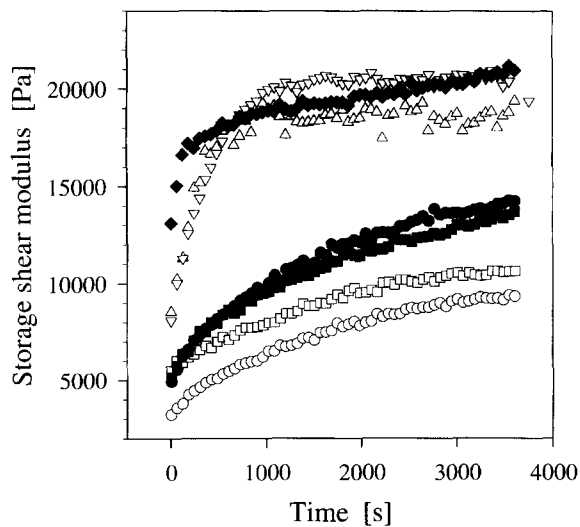


**Figure 9** Changes of storage and loss shear modulus during harmonic oscillation, i.e. stage two in the sequence of three (see Figure 7). (○ and □) B1 presheared for 63 and 622 s, respectively; (△ and ▽) B2 for 63 and 127 s; (● and ■) C4 for 64 and 312 s; (◆) C5 for 64 s

**Figure 10** Changes of storage and loss shear modulus during harmonic oscillation, i.e. stage two in a sequence of three (see Figure 7). The samples were first presheared to their individual viscosity minimum. The materials are: B1 (PIB1/PE, 53.6/46.4) □, B2 (PIB1/PE, 73.0/27.0) △, C1 (PIB1(W), 95.6(4.4)) ▲, C3 (PE(W), 95.0(5.0)) ○, C4 (PIB1/PE(W), 52.2/45.5(2.3)) ■, C5 (PIB1(W)/PE, 70.8(3.1)/26.1) ●, C6 (PIB1(W)/PE, 32.8(1.4)/65.8) ◆, C7 (PIB1(W)/PE, 11.4(0.5)/88.1) ▽.

points localised stress-concentrations should appear that might speed up the PE breakup accountable for the more rapid stiffness increase. PIB extraction of a C5 sample annealed for 1 h gave a coherent residue with lots of cluster-formed PE particles. Due to the slightly higher surface energy of PE it continues to cover the whisker surfaces, which accounts for the coherence of the sample. However, a steady unzipping of small PE domains takes place, which reduces the strength of the minority structure that eventually should lose its coherency.

Control of the weight loss of the PIB-extracted sample seen in Figure 12a gave 51.72% weight loss. If all PIB had been extracted 51.74% should have been lost. This is a good quantitative indication of the degree of co-continuity. As a comparison, the weight loss of the Brabender-compounded sample was 49.94%.

The start-up viscosities of the third stage of the three-step experiment are reported in Figure 13. As mentioned above, this is the average viscosity from 0.9 to 5 s. The limiting lines are given by the two morphological extremes, the lamellar<sup>17</sup> and the parallel perpendicular (rule of mixtures) structures. C4 is again close to the rule of mixture limit, suggesting the structure of an interpenetrating polymer

network (IPN). The B2 blend has much higher viscosity than its whisker-filled equivalent, probably due to the longer time required for the dispersed spherical particles to collide and create a stratified structure. Percolation is reached at much lower volume content if the particles have an aspect ratio. Already the moderate 3.1 v/o whisker loading reduces the percolation threshold of the PE phase to form a network throughout the sample, which is obvious from the coherence of an annealed extracted C5 sample.

The third step showed the same viscous response to prolonged steady shear as the first step for the different blends and composites, i.e. a similar behaviour as in Figure 2. Sequences of steady dynamic–steady dynamic–...–steady with shear to the viscosity minimum and short dynamic periods gave an equally repeatable rheological response before the degradation onset. These observations suggest that the morphological changes are repeatable.

Blends of poly(styrene-co-acrylonitrile)/polyamide 6 (SAN/PA6) were also studied. In these blends the whiskers are known to bring continuity to the minority PA6 phase,

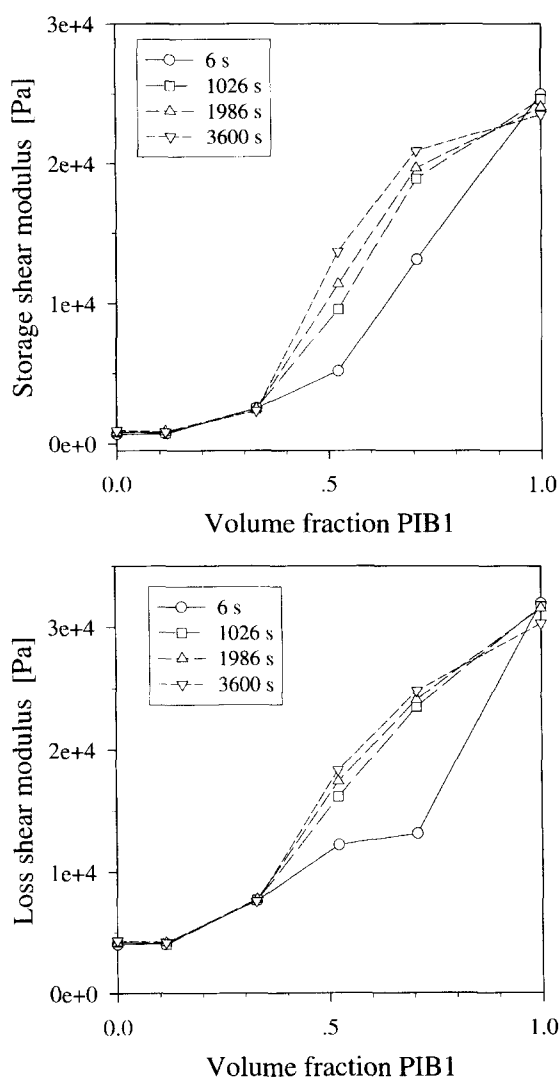


**Figure 11** Compilation of stiffness data from *Figure 10* after certain elapsed oscillation times of the composites

whereas they do not change the dispersed SAN phase in blends with a majority PA6 component<sup>7</sup>. The morphological stability of the co-continuous SAN/PA6-W composites has been found to be rather poor<sup>7</sup> at high shear rates. Thus, a reference system is offered. The same three-step procedure was employed for these blends and composites. *Figure 14* shows how the pattern is repeated also for this blend (C10) when whiskers are added. The interaction between SAN and whiskers is much weaker than between PA6 and whiskers. Thus, C11 maintains its dispersion-like phase structure with SAN spheres in a whisker-filled PA6 matrix.

## CONCLUSIONS

A very simple and convenient method for studies of morphological changes in polymer blends taking place during/after processing is presented. By this method, employing a sequence of steady and dynamic shear, it was shown how rheothermal response correlated with morphological evolution for a series of pure and whisker-filled PIB/PE blends. During the thermal stability time of these blends, morphological recoveries after steady shear and approach of morphological

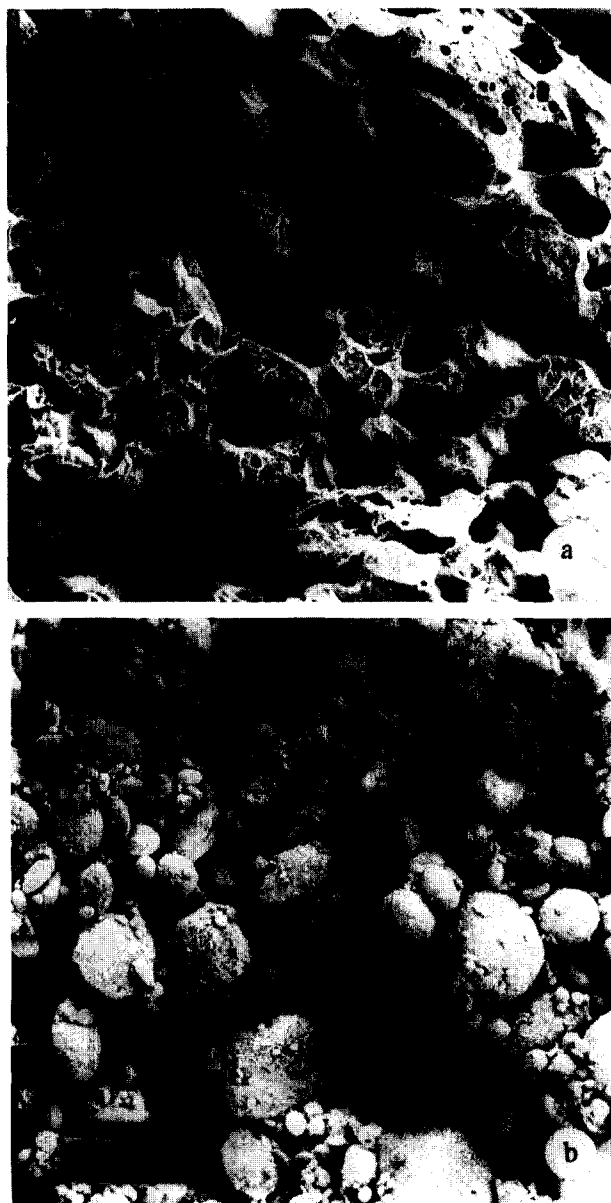


**Figure 12** SEM micrographs of fracture surfaces of PIB1/PE blends in volume ratios (a) 53.6/46.4 (B1) sheared 72 s at  $1 \text{ s}^{-1}$  and (b) 73.0/27.0 (B2), 62 s. Sample (b) is the residue after repeated centrifugation and cyclohexane-washing. The steady shear was followed by a 1-h rest for both samples. The arrow indicates the radial direction of the disc-shaped sample

equilibrium was seen. However, this time was insufficient for the whisker-filled blends to approach their morphological equilibrium state after a similar rheothermal history. Close to equal volume fractions of stable interpenetrating polymer network structures were formed, which were run to perfection by annealing.

## ACKNOWLEDGEMENTS

We would like to thank Professor Staffan Toll for valuable discussions. The Swedish National Board for Industrial and Technical Development (NUTEK) is also gratefully acknowledged for financial support within the framework of the material consortium 'Interfacial Interactions in Polymeric Systems'.

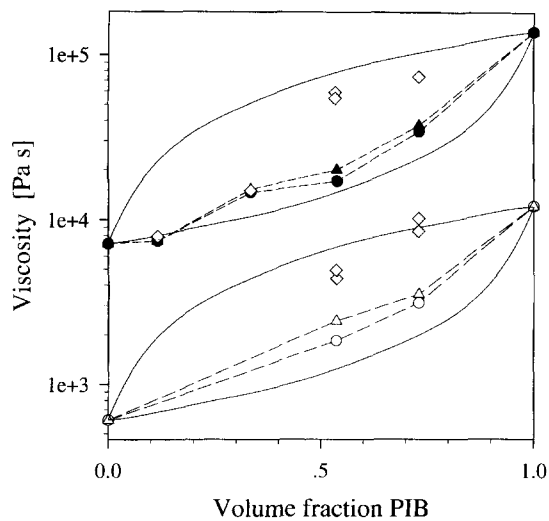


**Figure 13** Viscosity of unfilled plastics and blends in the lower part, which have been sheared to their minimum (open circles) and plateau (open triangles) viscosities. The composite viscosities (black symbols) have been shifted 10 times upwards. The black circles and triangles are equivalent to corresponding unfilled ones and the grey symbols represent the start-up viscosity of the third stage in the three-step sequence. The upper and lower limiting lines represent the rule of mixtures and a lamellar morphology according to Carriere and Ramanathan<sup>18</sup>

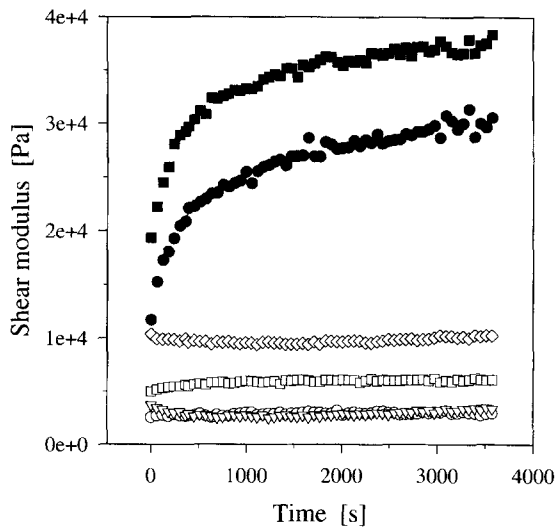


**Figure 14** Changes of storage ( $G'$ ) and loss ( $G''$ ) shear modulus during harmonic oscillation of SAN/PA6 blends and composites. These second steps in the three-step sequence were preceded by 62 s of steady shear at  $1 \text{ s}^{-1}$  shear rate. The symbols referring to  $G'$  and  $G''$  for blend B3 (SAN/PA6, 70/30 w/o) are open circles and squares, for composite C10 (SAN/PA6-W, 49/21-30) filled circles and squares and finally for C11 (SAN/PA6-W, 21/49-30) triangles and diamonds

## REFERENCES

1. Han, C. D., *Multiphase Flow in Polymer Processing*, Academic Press, New York, 1981.
2. Utracki, L. A., in *Rheological Measurement*, Ch. 15, ed. A. A. Collyer and D. W. Clegg. Elsevier Applied Science, London, 1988.
3. A.A. Collyer, in *Rheology and Processing of Liquid Crystal Polymers*, Ch. 6, ed. D. Acierno and A. A. Collyer. Chapman & Hall, London, 1996.
4. Quintens, D., Groeninckx, G., Guest, M. and Aerts, L., *Polym. Eng. Sci.*, 1990, **30**(22), 1474.
5. Quintens, D., Groeninckx, G., Guest, M. and Aerts, L., *Polym. Eng. Sci.*, 1991, **31**(16), 1207.
6. Quintens, D., Groeninckx, G., Guest, M. and Aerts, L., *Polym. Eng. Sci.*, 1991, **31**(16), 1215.
7. Persson, A.L. and Bertilsson, H., *Composite Interfaces*, 1996, **3**(4), 321.
8. Ljungqvist, N., Hjertberg, T., Persson, A. L. and Bertilsson, H., *Composite Interfaces*, 1997, **5**(1), 11.
9. Han, C. D., *Multiphase Flow in Polymer Processing*, Ch. 1. Academic Press, New York, 1981.
10. Persson, A. L. and Bertilsson, H., *Polymer*, in press.
11. Mekhilef, N. and Verhoogt, H., *Polymer*, 1996, **37**(18), 4069.
12. Jordhamo, G.M., Manson, J.A. and Sperling, L.H., *Polym. Eng. Sci.*, 1996, **26**(8), 517.
13. Takahashi, Y. and Noda, I., in *Flow-Induced Structure in Polymers*, Ch. 10, ed. A. I. Nakatani and M. D. Dadmun. ACS Symposium Series 597, ACS, Washington, DC, 1995.
14. La Mantia, F. P., in *Thermotropic Liquid Crystal Polymer Blends*, Ch. 4, ed F. P. La Mantia. Techno Publ., Lancaster, USA, 1993.
15. La Mantia, F. P., Titomanlio, G. and Valenza, A., in *Thermotropic Liquid Crystal Polymer Blends*, Ch. 5, ed. F. P. La Mantia. Techno Publ., Lancaster, USA, 1993.
16. Grassie, N., in *Polymer Science*, Vol. 2, Ch. 22, ed. A. D. Jenkins. North-Holland Publ. Company, London, 1972.
17. Quackenbos, H.M., *Polym. Eng. Sci.*, 1966, **6**, 117.
18. Carriere, C.J. and Ramanathan, R., *Polym. Eng. Sci.*, 1995, **35**(24), 1979.